Journal of Dental Sciences 20 (2025) 154–163

Available online at www.sciencedirect.com

ScienceDirect

journal homepage: www.e-jds.com

Original Article

2,3,5,4′-tetrahydroxystilbene-2-O-β-D-glucoside–stimulated dental pulp stem cells-derived exosomes for wound healing and bone regeneration

Tzu-Yu Lin [a,b†], Tung-Yung Huang [b,c†], Hsien-Chung Chiu [d], Yao-Yu Chung [b,c], Wei-Chun Lin [a,c,e], Hung-Yun Lin [f], Sheng-Yang Lee [a,b,c*]

[a] *Department of Dentistry, Wan-Fang Medical Center, Taipei Medical University, Taipei, Taiwan*
[b] *School of Dentistry, College of Oral Medicine, Taipei Medical University, Taipei, Taiwan*
[c] *Center for Tooth Bank and Dental Stem Cell Technology, Taipei Medical University, Taipei, Taiwan*
[d] *Department of Periodontology, School of Dentistry, National Defense Medical Center and Tri-Service General Hospital, Taipei, Taiwan*
[e] *School of Dental Technology, College of Oral Medicine, Taipei Medical University, Taipei, Taiwan*
[f] *Graduate Institute of Cancer Biology and Drug Discovery, College of Medical Science and Technology, Taipei Medical University, Taipei, Taiwan*

Received 26 August 2024; Final revision received 18 September 2024
Available online 27 September 2024

KEYWORDS
Human dental pulp stem cells (hDPSCs);
2,3,5,4′-tetrahydroxystilbene-2-O-β-D-glucoside (THSG);
Exosomes;
Proteomics approach;
Wound healing;

Abstract *Background/purpose:* -2,3,5,4′-tetrahydroxystilbene-2-O-β-D-glucoside (THSG) is a bioactive component in the Chinese herb Polygonum multiflorum, recognized for its anti-inflammatory and lipid-lowering properties. Human dental pulp stem cells (hDPSCs) have excellent capabilities in tooth regeneration, wound healing, and neural repair. The exosomes (Exo) released by hDPSCs contain bioactive molecules that influence cell proliferation, differentiation, and immune responses. Therefore, we aimed to unveil the potential of THSG-Exo and evaluate its regenerative capabilities through the *in vitro* experiment and rat bone defect model.
Materials and methods: The effects of hDPSC-derived exosomes, with or without THSG treatment, on repair and bone regeneration were evaluated through *in vitro* and *in vivo* studies. Finally, we conducted a proteomic analysis to meticulously compare the compositional contents of the two types of exosomes.
Results: In vitro data showed that 10 and 100 μM THSG-Exo enhanced cell proliferation and osteogenic differentiation, reducing wound size to 40 % of its original size. In our maxillary bone

* Corresponding author. School of Dentistry, College of Oral Medicine, Taipei Medical University, No. 250, Wuxing St., Xinyi Dist., Taipei, 11031, Taiwan.
E-mail address: seanlee@tmu.edu.tw (S.-Y. Lee).
† These authors contributed equally to this study.

https://doi.org/10.1016/j.jds.2024.09.010

Osteogenic regeneration

defect rat model, THSG-Exo significantly increased bone volume, trabecular thickness, and bone density in the bone defect area. In addition, proteomic analysis of THSG-Exo revealed diverse proteins linked to bone differentiation and tissue repair, including bone morphogenetic protein-1 (BMP-1) and tumor necrosis factor (TNF)-α-stimulated gene 6 (TNFAIP6). Our searches in functional databases revealed that THSG-Exo is involved in numerous biological pathways.
Conclusion: THSG-Exo enhanced cell proliferation, wound healing, and osteogenesis *in vitro*, while also expediting tissue repair and bone regeneration *in vivo*. The protein diversity of THSG-Exo contributes significant value in both basic and regenerative medicine.

Introduction

Alveolar bone repair post-trauma, surgery, or periodontal breakdown is intricate, especially when surgical complications or chronic diseases are present, making gingival wound healing challenging. Clinicians need to manage inflammation, curb bacterial infection, and minimize invasive procedures to successfully repair oral and maxillofacial injuries and prevent issues like secondary tissue damage. Tissue engineering, using cell therapy for immune modulation and tissue repair, is increasingly applied in regenerative medicine for reconstruction or functional restoration.[1,2]

The limitations of cell therapy have led researchers to increasingly focus on the paracrine effects of mesenchymal stem cells (MSCs).[3,4] Research on conditioned medium has shown that MSC-derived extracellular vesicles (EVs) are crucial in cell therapy, mediating immune responses, disease progression, and drug delivery.[5] Dental stem cells are a valuable resource for regenerative therapies because they are readily accessible through minimally invasive collection methods.[6,7] In particular, dental pulp stem cells (DPSCs) exhibit remarkable proliferation and multilineage differentiation abilities, rendering them suitable for immune modulation, neural repair, and wound healing purposes.[8] Relative to MSC-EVs from other sources, DPSC-EVs reportedly exhibit superior therapeutic efficacy in dental diseases, neurological disorders, and wound healing.[9] *In vivo* experiments have also demonstrated that MSC-EVs play a crucial role in bone defect repair.[10] However, the regenerative ability of DPSC-EVs remains to be explored.

Notably, 2,3,5,4′-Tetrahydroxystilbene-2-O-β-D-glucoside (THSG) is a water-soluble polyphenolic compound that can scavenge free radicals and has antilipidemic properties. Studies show that THSG boosts osteogenic differentiation in hDPSCs and accelerates bone formation in a rat bone defect model.[11,12] It may regulate osteogenic differentiation by inhibiting the expression of KDM5A.[13] Cell therapy success depends on stem cell-secreted substances, and EVs from hDPSCs may promote bone healing. Research shows THSG-stimulated hDPSCs culture medium enhances wound healing in human skin and gingival fibroblasts (HGFs).[14] Therefore, we investigated whether THSG-stimulated hDPSCs exosomes could improve oral wound healing and enhance osteogenic differentiation in alveolar bone defects.

Materials and methods

Reagents and cell culture

We maintained hDPSCs in low-glucose Dulbecco's modified Eagle's medium (10-014-CM, Corning, NY, USA) with 10 % fetal bovine serum (FBS) and 1 % penicillin–streptomycin (Invitrogen, Grand Island, NY, USA). THSG was extracted as previously described and dissolved in dimethyl sulfoxide (Invitrogen) for cell treatment.[11,15] The other cell cultures are presented in the supplementary data.

Preparation of conditioned medium

The hDPSCs were cultured in growth media with medium containing 0.25 % stripped FBS for cell starvation for 1 day. To enhance the stimulation, 100 μM THSG was further evaluated based on previous study.[14] The cells were either treated or not treated with 10 or 100 μM THSG in 0.25 % stripped FBS medium for 48 h. Other experimental procedures for the purification of conditioned medium are provided in the supplementary data.

Isolation and identification of hDPSC-derived exosomes

For tangential flow filtration (TFF), we used a KrosFlo Map.03 Cross Flow TFF pump (Spectrum Laboratories, Rancho Dominguez, CA, USA) fitted with a 300-kDa molecular weight cut-off mPES hollow fiber MidiKros filter module. The control-CM and THSG-CM were aspirated from a conical bottle, pumped through the hollow fiber system, and recirculated into the conical bottle. The pressure of the pump system was monitored using KrosFlo digital pressure transducers and a monitor (Spectrum Laboratories). Adjustable clamps were used to maintain a low transmembrane pressure of 5 PSI, which minimized the loss of small exosomes into the permeate. To achieve buffer exchange and remove any remaining phenol red, the concentrated solution was washed with 10 volumes of 1 × PBS. Finally, the exosomes obtained from the control-CM and THSG-CM were sterilized by loading them in 0.22-μm syringe filters. For the identification of exosomes, we used transmission electron microscopy (TEM), particle size

analysis, and surface antigen detection. Detailed procedures are provided in the Supplementary data.

Cell viability assay

HGFs and MC3T3 cells were seeded at cell densities of 1000 and 3000 cells per well, respectively, in 96-well culture plates containing growth medium and then incubated for 24 h at 37 °C in a 5 % CO_2 environment. Subsequently, the medium was replaced with 5 % stripped serum for cell starvation, and then the THSG-Exo (10 μM, 100 μM) were added to the medium with 0.25 % stripped FBS; after 0, 3, and 5 days of continuous culture, the medium was replaced with 10 % CCK-8, and incubation proceeded at 37 °C for 1—4 h; the absorbance was measured hourly with a VersaMax microplate reader (Molecular Device, San Jose, CA, USA) at a wavelength of 450 nm.

Wound healing assay

For our wound healing assay, we first placed a culture-insert 2 well (ibidi GmbH, Martinsried, Germany) into a 6-cm cell culture dish and then seeded the HGF cells at a density of a 2.5×10^6 cells/cm^2. Photographs of the wound healing process were taken on days 0, 6, and 9 of culture. The size of the wound healing area was analyzed and calculated using Image J software (version 1.52a, NIH, USA). Detailed experimental procedures are presented in the Supplementary data.

Alizarin red staining

MC3T3 cells were cultured at a density of 1×10^5 cells/well in 12-well culture plates in MEM-α with 10 % FBS until 80 % confluence was achieved. Subsequently, the growth medium was replaced with mineralization medium (MEM-α medium containing 50 μM ascorbic acid, 10 nM dexamethasone, 20 mM β-glycerophosphate; Sigma—Aldrich, St. Louis, MO, USA) containing exosomes. Thereafter, the medium was changed every 2 days. After 1, 2, and 3 weeks of cultivation in each treatment, the hDPSCs were washed with PBS and fixed with 4 % paraformaldehyde (Sigma—Aldrich). The cells in the culture plate were stained with 2 % Alizarin Red S (Catalog No.: TMS-008-C, Merck Millipore, St. Louis, MO, USA) for 20 min. Finally, distilled water was used to remove the stained background from each well, and photographs were taken for documentation.

Rat alveolar bone defect model

In the first procedure, bilateral maxillary first molars were extracted and allowed to heal for 4 weeks (Fig. S1). In the second surgery, a 2.0 mm diameter, 0.5 mm width, and 1 mm depth alveolar bone defect was created in the healed bone to quantify and confirm defect consistency. The rats were randomly divided into the following 5 groups: PBS, low-dose DPSC-Exo, high-dose DPSC-Exo, low-dose THSG-Exo, and high-dose THSG-Exo (3 rats/group). In the PBS group, PBS and Matrigel were placed in the alveolar bone defect, whereas in the DPSC-Exo and THSG-Exo groups, approximately 1×10^5 or 1×10^6 exosomes and Matrigel were placed in the bone defect. The remaining steps for the rat alveolar bone defect model are provided in the supplementary data.

Radiographic analysis of hard tissue with micro-CT

Detailed experimental procedures to assess bone status are presented in the Supplementary data.

Osteoblast and immunohistochemical analysis

Three antibodies were used in the immunohistochemistry (IHC) assay: proliferating cell nuclear antigen (PCNA), osteopontin (OPN), and vascular endothelial growth factor (VEGF). The procedures for analyzing osteoblasts are detailed in the supplementary data.

Proteomics analysis

Complete exosome proteomics involved three steps: gel-assisted digestion, LC-MS analysis, and protein identification, with details in the Supplementary data.

Statistical analysis

Data were analyzed using SPSS version 19.0 (SPSS Inc., Chicago, IL, USA). One-way analysis of variance, followed by the Tukey—Kramer multiple comparison test, was conducted. $P < 0.05$ indicated statistical significance.

Results

Characterization of exosomes obtained through TFF

The transmission electron microscope (TEM) analysis revealed that the membranes of the exosomes, obtained through TFF, were spherical and remained intact; these characteristics are similar to those of exosomes obtained using the gold standard ultracentrifugation method (Fig. 1A). After tunable resistive pulse sensing (TRPS) analysis, the sizes of the fresh and lyophilized samples were 100—250 nm and 60—150 mm (Fig. 1B), respectively, indicating a marked size difference. Flow cytometry revealed that the expression levels of exosome marker CD9 were higher in the THSG-Exo than in the DPSC-Exo (Fig. 1C). Stimulation of hDPSCs with THSG can prompt an increased production of exosomes.

THSG-Exo enhanced cell proliferation of HGFs and MC3T3 cells

HGFs cultured with 10 μM THSG-Exo showed a significant increase in proliferation on day 5, while 100 μM THSG-Exo did not (Fig. 2A). By contrast, MC3T3 cells cultured with THSG-Exo (100 μM) exhibited a significant increase in cell proliferation on day 3; THSG-Exo (10 μM) did not have this effect (Fig. 2B). The limited proliferation effect of 10 μM THSG-Exo in MC3T3 cells may be due to high osteogenic differentiation rather than proliferation.

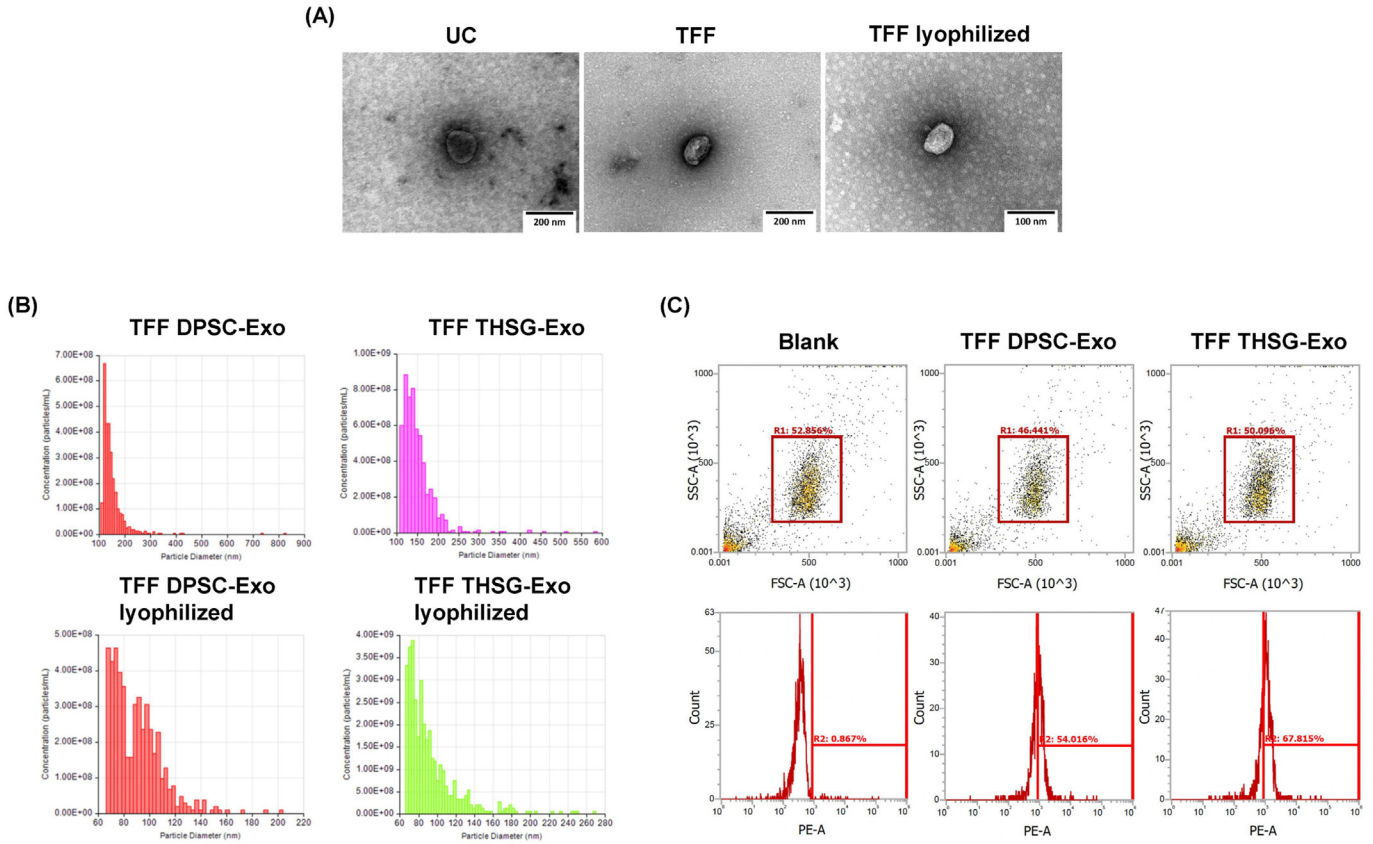

Figure 1 **Identification of exosome characteristics.** (A) The TEM image sequence for the experimental conditions is UC (ultracentrifugation), TFF (tangential flow filtration), and TFF lyophilized. The exosomes appeared as cup-shaped structures with a size of 50—150 nm. (B) Two types of exosome samples (DPSC- and THSG-exosome) were assessed by TRPS. The upper panel is the fresh group, and the lower panel is the lyophilized group. (C) Exosome samples were labeled with anti-CD9 antibodies and subsequently analyzed by flow cytometry.

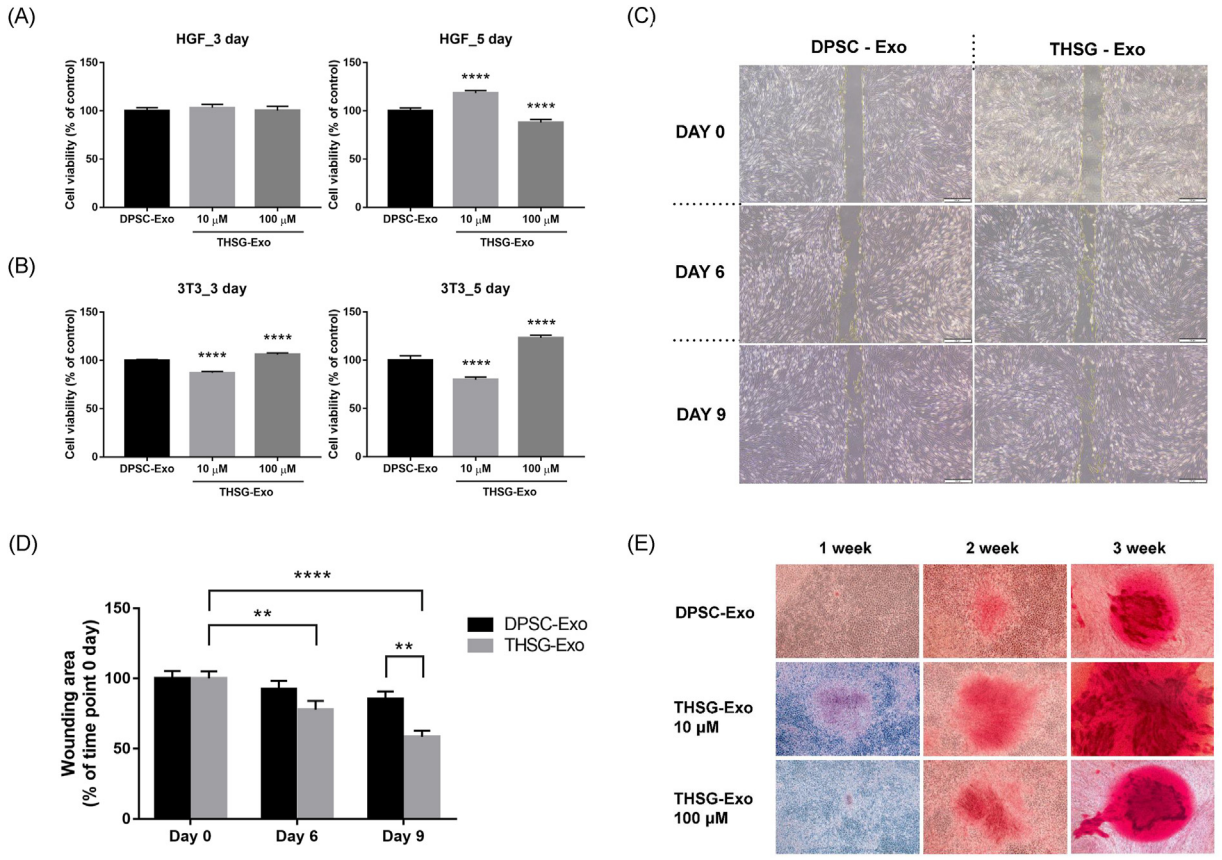

Figure 2 Influence of exosomes on the cellular functionality of HGF and MC3T3. (A and B) Assessing the impact of THSG-exosome concentrations on the cell viability of HGF and MC3T3 cells. (C) Representative images obtained from the wound healing assay of HGF cells. (D) The bar graph illustrated the wounding area percentage at indicated time points during the scratch wound assay. The number of independent studies (n) = 3. ****$P < 0.0001$ compared with the control or other conditions. (E) ARS staining of MC3T3 cells cultured for 21 Days in osteogenic induction microenvironments with THSG-exosomes.

THSG-Exo accelerated wound healing rate of HGFs

Because 10 μM THSG-Exo stimulated cell proliferation, we used HGFs to evaluate whether exosomes can accelerate wound healing. By day 6, wounds in HGFs treated with THSG-Exo were smaller than those treated with DPSC-Exo, with slight intercellular connections observed (Fig. 2C). The wound area in the THSG-Exo group was significantly smaller than that in the DPSC-Exo group on day 9. The wound area calculation results are presented in Fig. 2D. The wound area of HGFs cultured with THSG-Exo gradually decreased from days 6—9. On day 9, greater wound closure was observed in the THSG-Exo group than in the DPSC-Exo group. The wound area in the THSG-Exo group shrank to 40 % of its original size (Fig. 2D). These results indicate that THSG-induced exosomes significantly promote cell migration and wound healing in HGFs.

THSG-Exo enhanced osteogenic differentiation of MC3T3 cells

The MC3T3 cells were cultured in mineralization medium for 1, 2, and 3 weeks for osteoblast differentiation. In the group receiving THSG-Exo (10 μM), calcium nodules were observed on day 7, and in the second and third weeks, an increased number of larger dark red nodules was observed (Fig. 2E).

Micro-CT results of animal bone defect specimens

In our analysis, the degree of wound healing in the THSG-Exo group was superior to that in the DPSC-Exo group (Fig. 3A). We used software to analyze the micro-CT images of the large periodontal defect area and measured 4 values: the relative bone volume (BV/TV), trabecular thickness (Tb. Th), trabecular number (Tb. N), and trabecular spacing (Tb.Sp) (Fig. 3B). The THSG-Exo group had a higher BV/TV ratio than the PBS and DPSC-Exo groups, with even low-dose DPSC-Exo showing a higher ratio than PBS, indicating bone regeneration effects of exosomes (Fig. 3C). Similar trends were observed in terms of Tb. Th and Tb. N, with the THSG-Exo group having higher Tb. Th and Tb. N values than the PBS and DPSC-Exo groups did. Finally, we observed a significant difference in the Tb. Sp values between the 2 low-dose exosome groups; in addition, the Tb. Sp value in the high-dose THSG-Exo group was the lowest of those of all the groups, indicating that the degree of bone osteoporosis in the THSG-Exo group was lower than that in the DPSC-Exo group within the alveolar bony defect model (Fig. 3C).

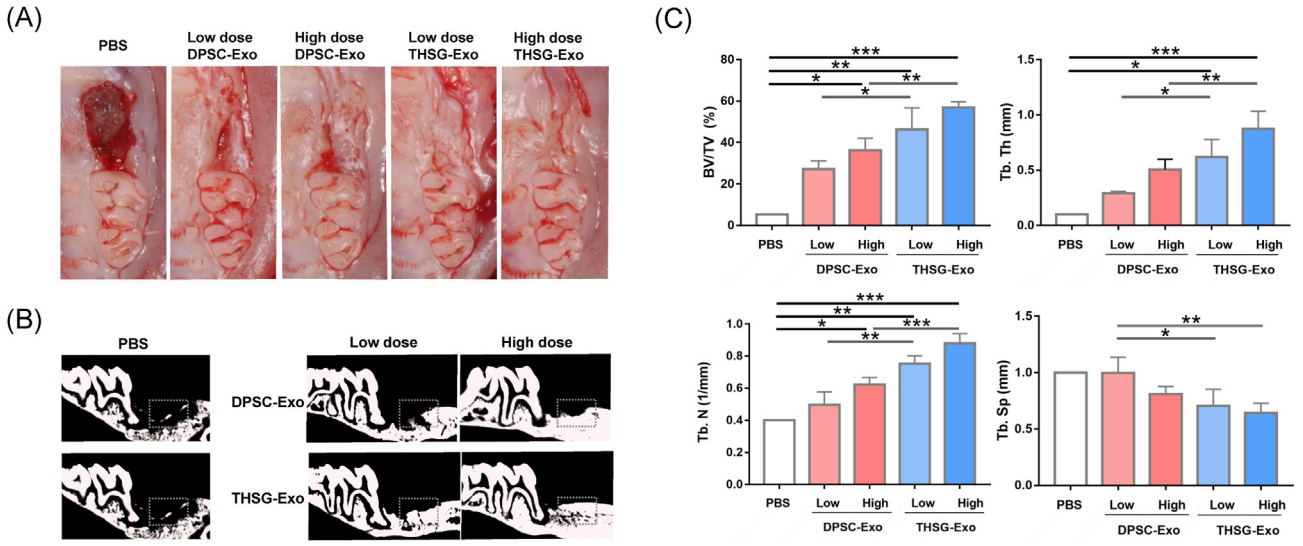

Figure 3 Evaluation of the exosomal influence on a rat alveolar bone defect model. (A and B) The status of gingival wound healing two weeks after surgery was assessed through photography and micro-CT. (C) Stimulating bone regeneration in rat bone defects with exosomes. Bone volume ratio (BV/TV), trabecular thickness (Tb. Th), trabecular number (Tb. N), and trabecular separation (Tb. Sp). The number of independent studies (n) = 3. ****$P < 0.0001$ compared with the PBS or other conditions. PBS: phosphate buffered saline.

Micro-CT analysis showed the THSG-Exo group had greater bone regeneration and less bone rarefaction compared to the DPSC-Exo and PBS groups.

Histological results of animal bone defect specimens

Our results indicated a greater increase in the number of osteoblasts in the 2 exosome groups than in the PBS group (Fig. 4A). In high doses, THSG-Exo led to the generation of more osteoblasts than did DPSC-Exo, confirming that the addition of THSG-Exo had a more favorable effect on new bone formation within the large bone defect. Moreover, the high dose of THSG-Exo outperformed the low dose. The IHC results indicated that both the low and high doses of THSG-Exo resulted in greater regeneration or osteogenic differentiation of cellular tissues than that which occurred in the other groups (Fig. 4B). The low-dose DPSC-Exo and THSG-Exo groups showed significantly higher OPN levels than the PBS group, suggesting these exosomes increased OPN expression (Fig. 4C, left). The THSG-Exo and the DPSC-Exo groups also differed significantly in terms of OPN expression levels, with dose-dependent characteristics. Similar trends were also observed for PCNA (Fig. 4C, middle). Thus, THSG-Exo increased PCNA and OPN levels, boosting cell proliferation and osteogenic functionality in alveolar bone defect tissues. The expression levels of VEGF were higher in high-dose than in low-dose THSG-Exo (Fig. 4C, right). However, the VEGF expression levels following both low-dose and high-dose DPSC-Exo treatment did not differ significantly from that in the PBS group. Although VEGF levels didn't significantly increase after DPSC-Exo treatment, it was still detectable in IHC images. Longer treatment may reveal differences in VEGF expression.

Proteome comparison between DPSC-Exo and THSG-Exo

The proteome results revealed that DPSC-Exo and THSG-Exo contained 180 and 280 proteins, respectively (Fig. 5A and Table S1). The 2 exosome groups shared 163 proteins, with 66 and 18 proteins being upregulated and downregulated, respectively, and 79 proteins exhibiting no significant differences. In these 2 sets of exosomes, we collectively identified 297 unique proteins, with THSG-Exo representing the majority. A Venn diagram revealed that DPSC-Exo had 17 unique proteins, constituting 5.74 % of the total. Following THSG stimulation, the THSG-Exo produced by hDPSCs had 117 unique proteins, accounting for 39.5 % of the total (Fig. 5A). The top 10 results for the 117 unique proteins in THSG-Exo across three categories in the GO database (cellular component, molecular function, and biological process) are shown in Fig. 5B: the first 3 results were related to the cellular component category, highlighting that these unique proteins are primarily associated with the composition of exosomes (Table S2); in the molecular function category, the most prominent pathways were extracellular matrix (ECM) structural constituent, calcium ion binding, and integrin binding, all of which are related to tissue regeneration and repair; and in the biological process category, we observed pathways involving the positive regulation of cell adhesion, cell migration, muscle cell differentiation, and angiogenesis, among others. Subsequently, we searched the Kyoto Encyclopedia of Genes and Genomes (KEGG) database for the 117 unique proteins, and found that they were associated with 26 biologically relevant pathways (Table S3). Five key pathways for regeneration and repair are ECM receptor interaction, focal adhesion, PI3K–Akt signaling, protein processing in the endoplasmic reticulum, and regulation of

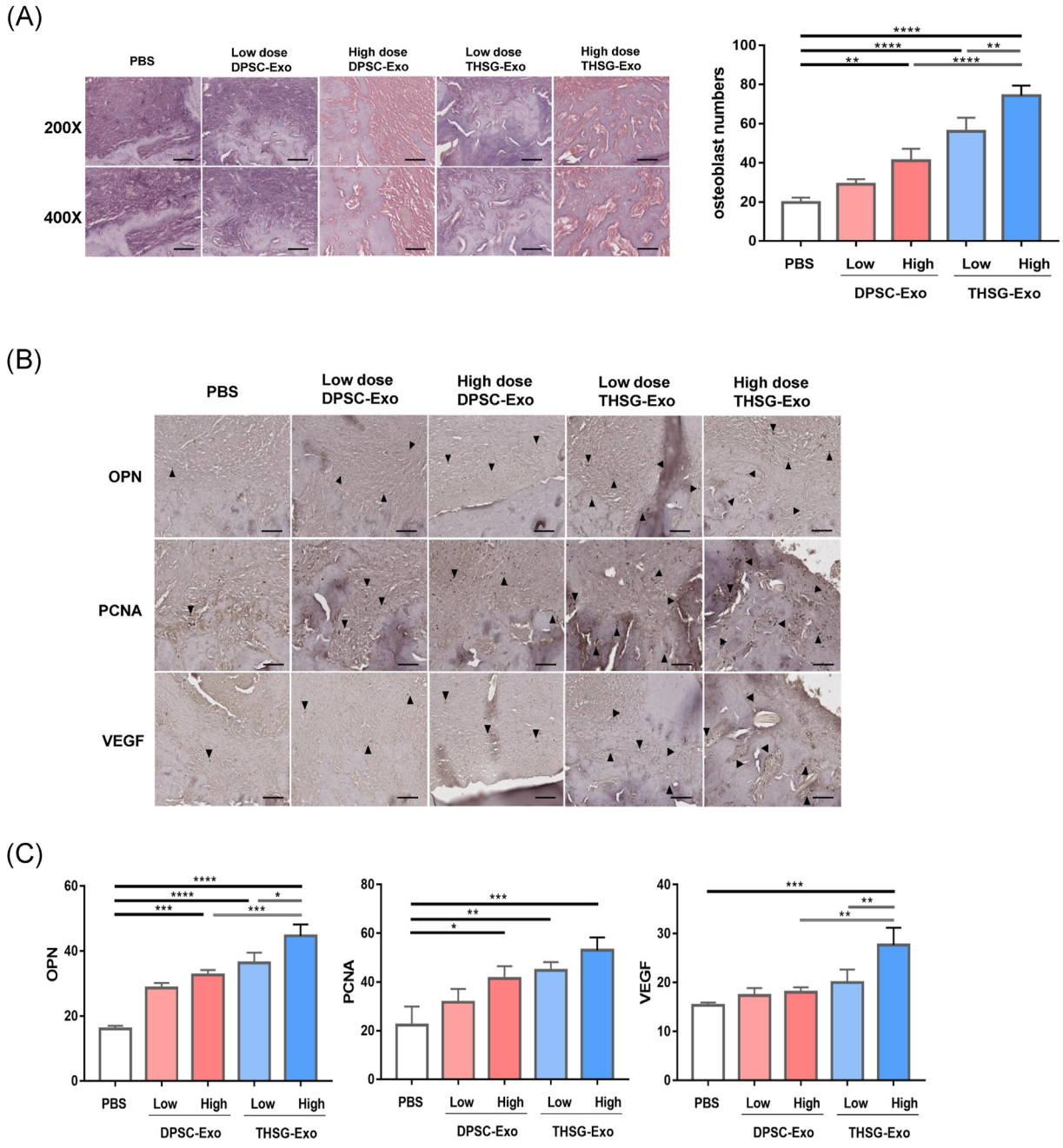

Figure 4 Histopathological analysis of the exosomal influence on a rat alveolar bone defect model. (A) Microscopic photographs are shown of 5 representative groups stained with hematoxylin and eosin (H&E) (200 ×, scale bar = 100 μm; lower panel: 400 ×, scale bar = 100 μm). A bar graph illustrates the number of quantified osteoblasts (right panel). (B) Microscopic photographs revealed the connective tissue area adjacent to the root and immediately above the newly formed alveolar bone (magnification: 200×; bar = 50 μm). Use IHC to observe the expression of proliferating cell nuclear antigen (PCNA), osteopontin (OPN), and vascular endothelial growth factor (VEGF) in connective cells adjacent to the new bone area (arrow). (C) Quantitative data of IHC on connective tissue were from PBS, DPSC-exosome (low and high dose), and THSG-exosome (low and high dose) samples. The number of independent studies (n) = 3. ****$P < 0.0001$ compared with the PBS or other conditions. PBS: phosphate buffered saline.

the actin cytoskeleton (related to integrin binding pathway) (Fig. 5B). Finally, we used the Cytoscape program to visualize the links between the KEGG and GO enrichment analyses (Fig. 5C). Visualization showed that THSG-Exo's unique proteins influence osteogenesis, wound healing, and tissue repair (Table 1).

Discussion

In this study, we elucidated the effects of THSG-induced exosomes derived from hDPSCs *in vitro* and *in vivo*. THSG-Exo (10 μM) significantly increased cell proliferation in HGF, but this effect was not observed in MC3T3 cells at the

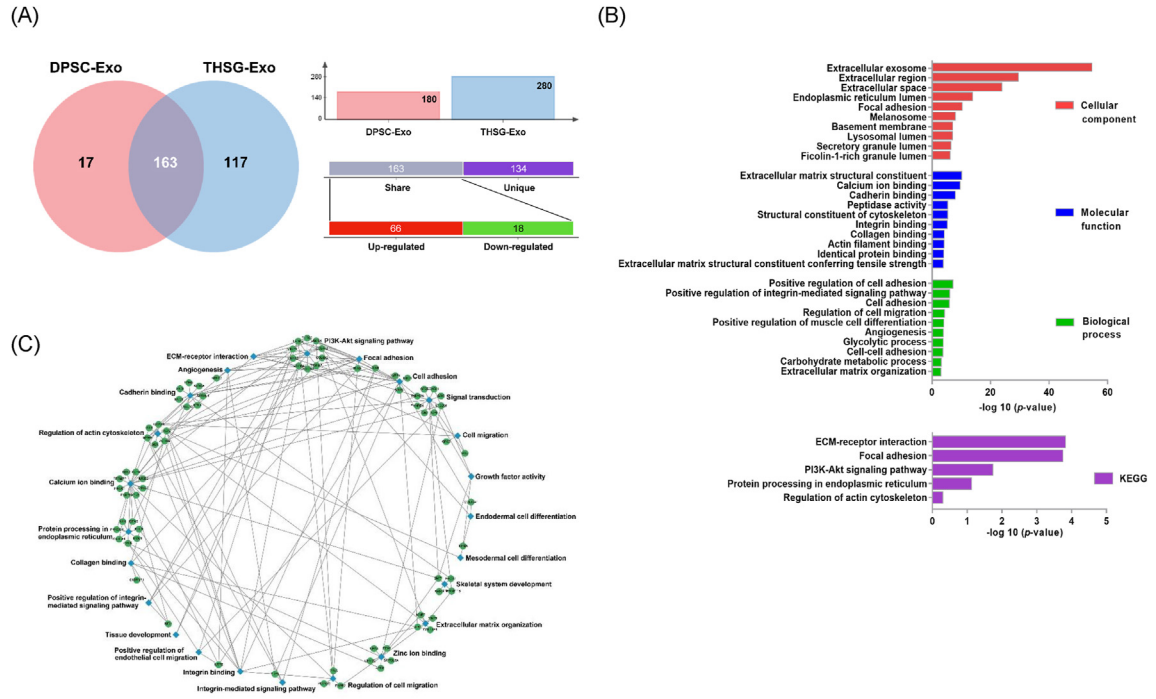

Figure 5 The proteome analysis results of THSG-induced hDPSCs exosomes. DPSC-Exo and THSG-Exo were both subjected to protein composition analysis using 1×10^9 exosomes. (A) Venn diagram of total proteins identified in the purified exosomes isolated using TFF between the DPSC and THSG groups. (B) The gene ontology (GO) enrichment and Kyoto encyclopedia of genes and genomes (KEGG) pathways analysis of unique proteins in THSG-exosome group. (C) Functional interaction networks analyzed by the Cytoscape plugin with unique proteins in the THSG-exosomes. (Sources URL, https://github.com/cytoscape/cytoscape.js; Version, 3.10.0). See Supplementary Table S1 for detailed protein information on both groups and the proteins they share.

Table 1 List of unique proteins in THSG-exosome associated with regenerative functions.

	Accession NO.	Gene	Protein
Osteogenesis	P13497	BMP-1	Bone morphogenetic protein 1
	Q15582	TGFBI	Transforming growth factor-beta-induced protein ig-h3
	O00300	TNFRSF11B	Tumor necrosis factor receptor superfamily member 11B
Wound healing	P03956	MMP-1	Interstitial collagenase
	P24043	LAMA2	Laminin subunit alpha-2
	P05556	ITGB1	Integrin beta-1
Tissue repair	P49767	VEGFC	Vascular endothelial growth factor C
	P01137	TGFB1	Transforming growth factor beta-1 proprotein

Accession No.: Accession number is based on the Uniprot database (https://www.uniprot.org/).

same dosage. The different effects of THSG-Exo concentrations on cell proliferation in HGFs and MC3T3 cells may be attributed to cell type specificity. Zhang et al. observed that bone marrow mesenchymal stem cell exosomes (BMMSC-Exo) induced cell proliferation in MC3T3 cells.[16] However, Shimizu et al. discovered that exosomes derived from DPSCs and gingival mesenchymal stem cells (GMSCs) did not have a proliferative effect in MC3T3 cells.[17] BMMSC-Exo, DPSC-Exo, and GMSC-Exo exhibit cell-specific responses in MC3T3 cells because of the distinct origins of the stem cells. *In vitro* experiments indicated that 10 μM THSG-Exo does not induce MC3T3 cell proliferation, likely due to involvement in other functions like osteogenic differentiation. Previous studies showed that stimulating human skin fibroblasts with ADSC-EV promoted cell proliferation and migration, increased MMP-1 expression, and phosphorylated AKT;[18,19] thus, adipose stem cell exosomes may accelerate wound healing in rat skin wounds through the PI3K–Akt pathway. Wang et al. also reported a significant increase in the expressions of MMP-1 and MMP-3 under the influence of exosomes.[20] In a mouse skin wound model, they achieved a reduction in scar formation and improved wound repair by increasing the ratio of MMP-3 to tissue inhibitor of metalloproteinase, thereby facilitating ECM remodeling. Another team used the secretome of HGFs to accelerate the healing of large skin wounds through the

secretome's anti-inflammatory effects, promotion of angiogenesis, and induction of collagen regeneration.[21] However, few studies have considered the promotion of wound healing by DPSC-Exo. Our proteomic findings highlight the PI3K—Akt pathway and MMP proteins in promoting wound closure in HGFs and rat gingival healing via THSG-Exo. In summary, THSG-Exo includes various unique proteins related to wound healing, consistent with our findings that THSG-induced hDPSCs exosomes demonstrate enhanced wound healing abilities.

Bone morphogenetic protein-2 (BMP-2) is an FDA-approved (US Food and Drug Administration) osteogenic factor.[22,23] Some research shows that BMP-2 is osteoinductive only at optimal doses,[24] while high doses cause inflammation and abnormal bone formation.[25] In this study, we found that THSG-Exo exhibit a greater bone-promoting effect than BMP-2 does. Lee et al. found that DPSC-Exo stimulated jawbone MSCs with osteogenic differentiation efficacy comparable to BMP-2.[26] We propose THSG-Exo as a potential alternative to BMP-2 for bone induction, with BMP-1 as a unique protein in THSG-Exo. Related studies have confirmed that enhancing its expression can promote osteogenic differentiation in bone marrow mesenchymal stem cells (BMSCs).[27] In addition to BMP-1, THSG-Exo include anti-inflammatory proteins such as tumor necrosis factor (TNF)-α-stimulated gene 6 (TSG-6 or TNFAIP6). It can compete with the receptor activator of nuclear factor kappa-B ligand on the surface of osteoclasts to inhibit bone resorption activity. *In vitro* experiments have highlighted the ability of TNFAIP6 to inhibit the activation of osteoclasts and promote osteoclast apoptosis.[28,29] Moreover, THY-1 (CD90) positively regulates osteogenic differentiation in bone marrow stromal cells and inhibits adipocyte differentiation in obese mice.[30] Our data show that THSG-Exo contains BMP-1 to activate osteoprogenitor cells and osteoprotegerin to inhibit bone-resorbing cells.

Most unique proteins in THSG-Exo possess diverse functional properties, such as neuropilin 2 (NRP2). It binds with VEGF, thereby participating in the growth of neuronal axons, vascular neogenesis, and other processes. Angiopoietin-1, an ECM glycoprotein, aids in regeneration and repair by inhibiting apoptosis, promoting migration, maintaining vascular integrity, and inducing angiogenesis and tissue remodeling.[31] Autotaxin (ATX), also known as ectonucleotide pyrophosphatase/phosphodiesterase family member 2, can promote cell migration and proliferation through lysophosphatidic acid receptor signaling. Additionally, it participates in angiogenesis and tissue repair induced by VEGF.[32]

THSG-Exo surpassed DPSC-Exo in *in vitro* and *in vivo* experiments for wound healing, osteogenic differentiation, and tissue repair. Both types of exosomes are water-soluble and stable, and can be used clinically with dressings for direct application on soft and hard tissues. THSG-Exo is particularly effective when combined with bone graft materials to address potential gingival atrophy after tooth extraction.

Declaration of competing interest

The authors have no conflicts of interest relevant to this article.

Acknowledgments

We acknowledge the helps from Prof. Ching-Chiung Wang. This study was supported by grants MOST110-2314-B-038-064-MY3 from Ministry of Science and Technology (MOST), Taiwan.

Appendix A. Supplementary data

Supplementary data to this article can be found online at https://doi.org/10.1016/j.jds.2024.09.010.

References

1. Han F, Wang J, Ding L, et al. Tissue engineering and regenerative medicine: achievements, future, and sustainability in asia. *Front Bioeng Biotechnol* 2020;8:83.
2. Zhang Y, Wu D, Zhao X, et al. Stem cell-friendly scaffold biomaterials: applications for bone tissue engineering and regenerative medicine. *Front Bioeng Biotechnol* 2020;8:598607.
3. Sun Q, Zhang Z, Sun Z. The potential and challenges of using stem cells for cardiovascular repair and regeneration. *Genes Dis* 2014;1:113—9.
4. Gorecka J, Kostiuk V, Fereydooni A, et al. The potential and limitations of induced pluripotent stem cells to achieve wound healing. *Stem Cell Res Ther* 2019;10:87.
5. Yong T, Wei Z, Gan L, Yang X. Extracellular-vesicle-based drug delivery systems for enhanced antitumor therapies through modulating the cancer-immunity cycle. *Adv Mater* 2022;34:e2201054.
6. Gronthos S, Mankani M, Brahim J, Robey PG, Shi S. Postnatal human dental pulp stem cells (DPSCs) in vitro and in vivo. *Proc Natl Acad Sci U S A* 2000;97:13625—30.
7. Huang GT, Gronthos S, Shi S. Mesenchymal stem cells derived from dental tissues vs. those from other sources: their biology and role in regenerative medicine. *J Dent Res* 2009;88:792—806.
8. Anitua E, Troya M, Zalduendo M. Progress in the use of dental pulp stem cells in regenerative medicine. *Cytotherapy* 2018;20:479—98.
9. Li Y, Duan X, Chen Y, Liu B, Chen G. Dental stem cell-derived extracellular vesicles as promising therapeutic agents in the treatment of diseases. *Int J Oral Sci* 2022;14:2.
10. Bei HP, Hung PM, Yeung HL, Wang S, Zhao X. Bone-a-petite: engineering exosomes towards bone, osteochondral, and cartilage repair. *Small* 2021;17:e2101741.
11. Chin YT, Hsieh MT, Lin CY, et al. 2,3,5,4'-tetrahydroxystilbene-2-o-beta-glucoside isolated from polygoni multiflori ameliorates the development of periodontitis. *Mediat Inflamm* 2016;2016:6953459.
12. Lin CY, Kuo PJ, Chin YT, et al. Dental pulp stem cell transplantation with 2,3,5,4'-tetrahydroxystilbene-2-o-beta-d-glucoside accelerates alveolar bone regeneration in rats. *J Endod* 2019;45:435—41.
13. Wei M, Jiang Y, Huang Y. TSG targeting KDM5A affects Osteogenic differentiation of bone mesenchymal stem cells induced by bone morphogenetic protein 2. *J Healthc Eng* 2022;2022:6472864.
14. Chin YT, Liu CM, Chen TY, et al. 2,3,5,4'-tetrahydroxystilbene-2-o-beta-d-glucoside-stimulated dental pulp stem cells-derived conditioned medium enhances cell activity and anti-inflammation. *J Dent Sci* 2021;16:586—98.
15. Tsai PW, Lee YH, Chen LG, Lee CJ, Wang CC. In vitro and in vivo anti-osteoarthritis effects of 2,3,5,4'-tetrahydroxystilbene-2-

o-beta-d-glucoside from polygonum multiflorum. *Molecules* 2018;23:571.
16. Zhang L, Jiao G, Ren S, et al. Exosomes from bone marrow mesenchymal stem cells enhance fracture healing through the promotion of osteogenesis and angiogenesis in a rat model of nonunion. *Stem Cell Res Ther* 2020;11:38.
17. Shimizu Y, Takeda-Kawaguchi T, Kuroda I, et al. Exosomes from dental pulp cells attenuate bone loss in mouse experimental periodontitis. *J Periodontal Res* 2022;57:162—72.
18. Zhang W, Bai X, Zhao B, et al. Cell-free therapy based on adipose tissue stem cell-derived exosomes promotes wound healing via the PI3K/akt signaling pathway. *Exp Cell Res* 2018;370:333—42.
19. Ren S, Chen J, Duscher D, et al. Microvesicles from human adipose stem cells promote wound healing by optimizing cellular functions via akt and erk signaling pathways. *Stem Cell Res Ther* 2019;10:47.
20. Wang L, Hu L, Zhou X, et al. Exosomes secreted by human adipose mesenchymal stem cells promote scarless cutaneous repair by regulating extracellular matrix remodelling. *Sci Rep* 2017;7:13321.
21. Ahangar P, Mills SJ, Smith LE, Gronthos S, Cowin AJ. Human gingival fibroblast secretome accelerates wound healing through anti-inflammatory and pro-angiogenic mechanisms. *NPJ Regen Med* 2020;5:24.
22. Gillman CE, Jayasuriya AC. FDA-approved bone grafts and bone graft substitute devices in bone regeneration. *Mater Sci Eng C* 2021;130:112466.
23. Boden SD, Zdeblick TA, Sandhu HS, Heim SE. The use of rhBMP-2 in interbody fusion cages definitive evidence of osteoinduction in humans: a preliminary report. *Spine* 2000;25:376—81.
24. Razzouk S, Sarkis R. BMP-2: biological challenges to its clinical use. *N Y State Dent J* 2012;78:37—9.
25. James AW, LaChaud G, Shen J, et al. A review of the clinical side effects of bone morphogenetic protein-2. *Tissue Eng Part B Rev* 2016;22:284—97.
26. Lee AE, Choi JG, Shi SH, He P, Zhang QZ, Le AD. DPSC-derived extracellular vesicles promote rat jawbone regeneration. *J Dent Res* 2023;102:313—21.
27. Su Z, He L, Shang H, Dai T, Xu F, Zhao J. Overexpression of bone morphogenetic protein-1 promotes osteogenesis of bone marrow mesenchymal stem cells in vitro. *Med Sci Monit* 2020; 26:e920122.
28. Yasuda H, Shima N, Nakagawa N, et al. Identity of osteoclastogenesis inhibitory factor (OCIF) and osteoprotegerin (OPG): a mechanism by which OPG/OCIF inhibits osteoclastogenesis *in vitro*. *Endocrinology* 1998;139:1329—37.
29. Simonet WS, Lacey DL, Dunstan CR, et al. Osteoprotegerin: a novel secreted protein involved in the regulation of bone density. *Cell* 1997;89:309—19.
30. Paine A, Woeller C, Huertas N, Garcia-Hernandez MD, Phipps R, Ritchlin CT. Thy1 is a positive regulator of osteoblast differentiation and modulates bone homeostasis in obese mice. *Faseb J* 2017;32:3174—83.
31. Brindle NPJ, Saharinen P, Alitalo K. Signaling and functions of angiopoietin-1 in vascular protection. *Circ Res* 2006;98: 1014—23.
32. Yung YC, Stoddard NC, Chun J. LPA receptor signaling: pharmacology, physiology, and pathophysiology. *J Lipid Res* 2014; 55:1192—214.